

SwissFEL LINAC COMMISSIONING STATUS, CURRENT PERFORMANCE AND FUTURE PLANS

P. Craievich* on behalf of the SwissFEL team
Paul Scherrer Institut, 5232 Villigen PSI, Switzerland

Abstract

SwissFEL, the hard x-ray free-electron laser facility at PSI, is in an advanced commissioning phase. The commissioning of the 5.8 GeV Linac started in 2016 and the first FEL pilot-experiments were performed at a reduced beam energy in the end of 2017. In 2018, it is foreseen to progressively increase the electron beam energy and photon energy up to the maximum design values, interleaved by several FEL pilot experiments. This paper gives an overview of the commissioning progress including the achieved machine performance and first operational experience.

INTRODUCTION

The newest large research facility at the Paul Scherrer Institute, the hard-X-ray free-electron laser SwissFEL [1] has recently commenced its scientific program with a series of pilot experiments. SwissFEL aims at delivering ultra-short coherent photon pulses through two beam lines called Aramis (hard X-rays, 1-7 Å) and Athos (soft X-rays, 6.5-50 Å). So far only the Aramis beam line has been commissioned with two experimental stations in operation, called Alvra and Bernina. Alvra is a multipurpose pump-probe station focusing on ultrafast biology and chemistry, while Bernina specializes in pump-probe crystallography for the study of ultrafast dynamics in solid matter, in particular strongly correlated systems, as well as structural biology.

The SwissFEL accelerator consists of an electron source, an S-band (3 GHz) booster linac and a C-band (5.7 GHz) main linac (Fig. 1). The electron source is a laser driven 2.5-cell S-band RF photoinjector gun. The electron bunches, with charge ranging between 10 and 200 pC, are longitudinally compressed in two stages at nominal energies of 300 MeV and 2.1 GeV, respectively. A higher-harmonic cavity (X-band, 12 GHz) linearizes the electron phase space before the first compression stage. The accelerated and compressed electron bunches are sent into the Aramis undulator line comprising 13 in-vacuum undulator modules of 4 m length each. A second undulator line, Athos, is currently under construction. It will be driven by 3 GeV electrons extracted in a switchyard halfway along the main linac. Table 1 lists the most important parameters of the SwissFEL facility.

This paper is an updated version of the contribution presented at the IPAC'18 [2] since new important results have been achieved between May and September 2018. SwissFEL linac reached its nominal electron beam energy of 5.8 GeV, first lasing with a photon energy of 9 keV and in the summer period other four pilot experiments were performed.

* paolo.craievich@psi.ch

STATUS OF C-BAND LINAC

The C-band main linac is the centrepiece of the SwissFEL accelerator defining the available electron and hence photon energy. It consists of a total of 26 RF modules, each providing a nominal accelerating voltage of 240 MV with four tuning-free copper structures [3,4]. Figure 2 shows a part of the tunnel with C-band accelerating structures. The effectively achieved accelerating voltages vary between 200 and 280 MV, depending on the conditioning states of the modules. In each station, an IGBT-switched solid-state modulator manufactured by Ampegon (first half of the linac) or ScandiNova (second half) drives an E37212 Toshiba klystron, which can furnish up to 50 MW for a duration of 3 μs. The RF pulse is compressed in a barrel-open-cavity (BOC) [5] before being delivered to the four structures via a precisely adjusted waveguide network. Currently 25 of the 26 stations are available for beam acceleration. One RF station in Linac 2 is currently used for the upgrade of the software system. In case of failure of one RF station in Linac 1 and/or Linac 3 there is enough RF power reserve in order to guarantee the operations. The delivered power is typically around to 80% of the maximum value.

Table 1: SwissFEL Main Parameters

| Parameter | Value |
|-----------------------|---------------|
| Photon wavelength | 0.1-5.0 nm |
| Photon energy | 0.25-12.4 keV |
| Pulse duration | 1-30 fs |
| Electron energy | 5.8 GeV |
| Electron bunch charge | 10-200 pC |
| Repetition rate | 100 Hz |

A campaign of measurements on the RF stations has been performed to characterize the actual stability of the klystron voltage. A high performance differential amplifier has been used for this scope. This implements a high stability low-noise voltage generator and a low overdrive recovery time comparator in order to accurately monitor the pulse-to-pulse reproducibility. The results of these measurements showed that pulse-to-pulse stability of the klystron high voltage are better than the specified value of 15 ppm.

After the conditioning periods dedicated for each RF station, typically from 3 to 4 weeks for RF stations, the SwissFEL Linac has reached the nominal electron bunch energy of 5.8 GeV required for Aramis beamline in September 2018. In the present configuration, the linac delivers 5.5 GeV for a total energy of 5.8 GeV (300 MeV from the injector linac). The beam energy is for a compressed bunch with off-crest op-

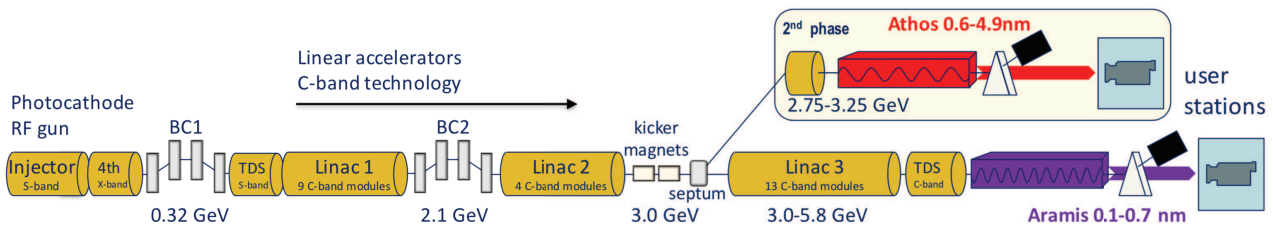


Figure 1: Schematic of SwissFEL accelerator layout (from Ref. [1] and [2]).



Figure 2: C-band accelerating structures in a part of the Linac 3.

eration in Linac 1. However, the operating energy is usually set according to the requirements for users' experiments and the working point of the single module is fixed to the maximum gradient achievable for a reliable operation. Figure 3 shows a panel with the distribution of the RF amplitudes and phases of the all RF stations including the two RF deflectors, SINDI01 and S30CB14, respectively. When less beam energy is required, some of the last structures are set off-line providing the redundancy that is very useful to ensure the operation for the users. The overall objective is to run the facility with a beam energy of 5.8 GeV at a repetition rate of 100 Hz by December of this year. Presently the repetition rate of the electron beam is 25 Hz. All C-band modules are systematically operated at 100 Hz. Recent tests with a low-charge beam at 25, 50 and 100 Hz basically demonstrated beam transport at these rates. After this first year

| Station | | MV | deg | Station | MV | deg |
|---------|-------------|-------|-------|---------|--------------|------------|
| SINEG01 | RF on beam | 7.2 | 90.0 | S20CB01 | RF on beam | 263.0 92.5 |
| SINSB01 | RF on beam | 68.5 | 90.0 | S20CB02 | RF on beam | 254.7 90.0 |
| SINSB02 | RF on beam | 65.4 | 90.0 | S20CB03 | RF on beam | 235.0 92.8 |
| SINSB03 | RF on beam | 99.0 | 67.9 | S20CB04 | INIT | 0.0 |
| SINSB04 | RF on beam | 99.0 | 67.8 | S30CB01 | RF on beam | 207.4 90.0 |
| SINXB01 | RF on beam | 19.9 | 264.4 | S30CB02 | RF on beam | 253.5 90.1 |
| SINDI01 | RF on delay | 4.2 | 256.0 | S30CB03 | RF on beam | 260.2 90.0 |
| S10CB01 | RF on beam | 243.8 | 77.8 | S30CB04 | RF on beam | 249.9 90.0 |
| S10CB02 | RF on beam | 242.9 | 77.8 | S30CB05 | RF on beam | 239.6 90.0 |
| S10CB03 | RF on beam | 249.2 | 77.8 | S30CB06 | RF on beam | 235.2 90.0 |
| S10CB04 | RF on beam | 212.7 | 77.8 | S30CB07 | RF on beam | 235.0 91.8 |
| S10CB05 | RF on beam | 262.3 | 77.8 | S30CB08 | RF on beam | 244.1 90.0 |
| S10CB06 | RF on beam | 253.6 | 77.8 | S30CB09 | RF on beam | 241.9 90.0 |
| S10CB07 | RF on beam | 228.5 | 78.5 | S30CB10 | RF on beam | 265.3 90.0 |
| S10CB08 | RF on beam | 193.5 | 77.8 | S30CB11 | RF on beam | 254.0 90.0 |
| S10CB09 | RF on beam | 237.7 | 77.8 | S30CB12 | Conditioning | 0.0 196.3 |
| | | | | S30CB14 | Conditioning | 85.0 2.0 |

Figure 3: Panel with the status of the RF stations.

of commissioning and operation, an optimization is under study to correct the major down-time sources, increase safety margins and redundancy and extend operating margins of the machine especially in terms of beam energy. The major source of downtime of the S-band and C-band stations is related to klystron arcs. The number has already been reduced

by optimizing the the operation point of the klystron. However, a modification of the ramping up procedure is under study to recover the beam operation after an arc. Analysis of the waveform of the anodic voltage and current after an arc are performed to study possible improvement of the recovery procedure.

To control the RF stations a new, in-house developed digital Low Level RF (LLRF) system measures up to 24 RF signals per station and performs a pulse-to-pulse feedback at a repetition rate of 100 Hz. Depending on the location along the machine the LLRF system controls the accelerating fields of up to 4 RF structures. The modular system consists of a common digital processing unit and a frequency dependent RF front-end which converts the different RF frequencies to a common intermediate frequency (IF). The topology of one C-band RF station includes the reference RF signal that is modulated by a vector modulator, amplified by one klystron and fed into four C-band accelerating structures. The input signal before and after the structure is measured and a vector sum is calculated which is required for a pulse-to-pulse feedback. The LLRF system is introduced to control all the RF stations to provide low noise RF phase and amplitude actuations and precise RF signal detections. Pulse-to-pulse feedbacks are applied on amplitude and phase at up to 100 Hz to achieve the RF stabilities. Drift calibration is required on critical RF signals used for feedback to improve the long-term stability of the system. Automation tools are also required to help the operators to easily setup and operate the RF stations [6, 7].

LINAC STABILITY

The beam stability requirements of the SwissFEL linac result in challenging specifications on the stability of the RF fields that can only be met using reliable and high performance modulators and LLRF systems (mentioned in the previous paragraph). FEL operation requires very high shot-to-shot stability of the electron beam energy, which for the S-band and C-band RF system translates in tight amplitude and phase jitter requirements as listed in Table 2 [8]. The achieved RF amplitudes and phases stabilities are also listed in Table 2. These values include the contribution of all components of the RF station. It is worthwhile noting that the relative beam energy jitter at the Linac end was measured at 4.7 GeV and was resulted approximately 0.01% that is well below the specified value of 0.05%.

Table 2: Pulse-to-pulse RF Phase and Amplitude Jitters (rms). Stability requirements are also indicated.

| RF station | RF phase | | RF amplitude | |
|------------|------------|-----------|--------------|-----------|
| | Meas. [°] | Spec. [°] | Meas. [%] | Spec. [%] |
| S-band | 0.010-0.04 | 0.018 | 0.01-0.02 | 0.02 |
| X-band | 0.05 | 0.072 | 0.04 | 0.02 |
| C-band | 0.018-0.04 | 0.036 | 0.01-0.02 | 0.02 |

SCHEDULE AND PILOT EXPERIMENTS

SwissFEL Aramis has now completed its second phase of pilot experiments, with one more phase to follow. The second phase lasted from June to August of this year and comprises again four pilot experiments, still to be carried out at reduced performance levels with respect to the SwissFEL design values. Figure 4 shows the schedule of the Aramis beamline in details.

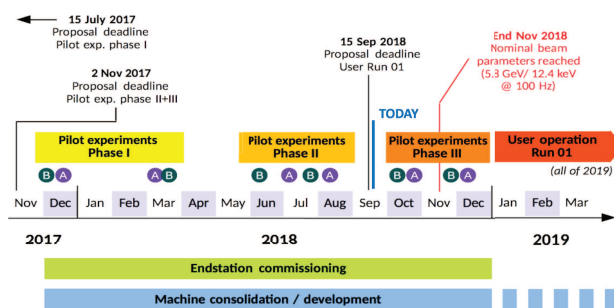


Figure 4: Schedule of the Aramis beamline (more details in [2]).

OUTLOOK

The third phase of the pilot experiments will last from October to December of this year and comprises again four experiments and the full performance level should be available (i.e., photons with up to 12.4 keV energy at 100 Hz pulse rate). This last pilot phase will be utilized to consolidate and characterize the machine performance before starting the first regular user operation run in early 2019 because in spite of the success and important milestones achieved so far, the accelerator and the beamlines are not yet in their final configurations. The commissioning of optical components, photon diagnostics and the experimental stations will proceed throughout 2018, in parallel with the machine development and consolidation program.

During the last shutdown in summer 2018 a pair of planar corrugated structures with orthogonal orientations were installed at the injector before the bunch compressor. For each device, three different corrugations, 1-m long, are mounted on a common support to manipulate and diagnose the bunch by self-inducing longitudinal and transverse wakefield. In one of these corrugations (*linearizer*), the self-induced wakes will partially compensate for the nonlinear

energy chirp imprinted by the RF field and the magnetic compression. In particular, we also want to verify that the quadrupole component of the wakefield that increases beam emittance can be effectively canceled with a pair of planar corrugations with orthogonal orientation [9]. However, each device has three different corrugation periods corresponding to as many impedances to carry on several studies as described in [10]. The routine use of such a device at lower energy in a user facility has to still be demonstrated, in particular we want to prove that it can be adjusted to different bunch lengths, charges and that it may be used to provide a more stable FEL beam. Figure 5 shows a drawing of the two passive devices installed on their girder.

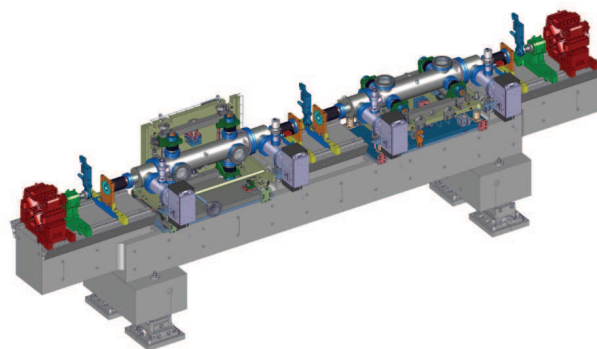


Figure 5: Drawing of the passive devices on their girder.

Athos Soft-X-Ray Line

The extensively redesigned Athos beam line [11] for the generation of soft X-rays in the range 250-1900 eV is currently under construction. Its main features are 16 Apple-X U38 undulators providing full polarization and transverse gradient control, with small magnetic chicanes between them to enable high-performance modes going by names such as "optical klystron", "high brightness" or "terawatt-attosecond" [12]. In addition, a larger magnetic chicane at the center of the undulator line will allow for two-color operation with controllable delay between the pulses up to 500 fs. A resonant kicker magnet system [13], custom-designed to divert the two bunches separated by 28 ns into the respective beam lines, was installed earlier this year and has recently undergone first tests diverting the second bunch to the Athos dogleg.

As a diagnostic tool, a X-band Transverse Deflection Structure (TDS) will be installed downstream of the undulators of the Athos beamline, which will allow to indirect measurement of the X-Ray pulse length by analysing the induced energy spread on the electron bunch due to the FEL process [14]. Furthermore, thanks to the variable polarization of the TDS [15] it will be possible to perform a complete characterization of the 6D phase space by means of measurements of bunch length, energy and transverse slice emittances (vertical and horizontal) [16]. Since several experiments at DESY (FLASH2, FLASHForward, SINBAD) are also interested in the utilization of such a X-band TDS

systems for high-resolution longitudinal diagnostics, a collaboration between DESY, PSI and CERN has been established to develop and build this advanced modular X-Band TDS system [17]. Figure 6 shows a mechanical drawing of a short version of the TDS constituted by 10 cells (number of cells of the actual prototype is 96).

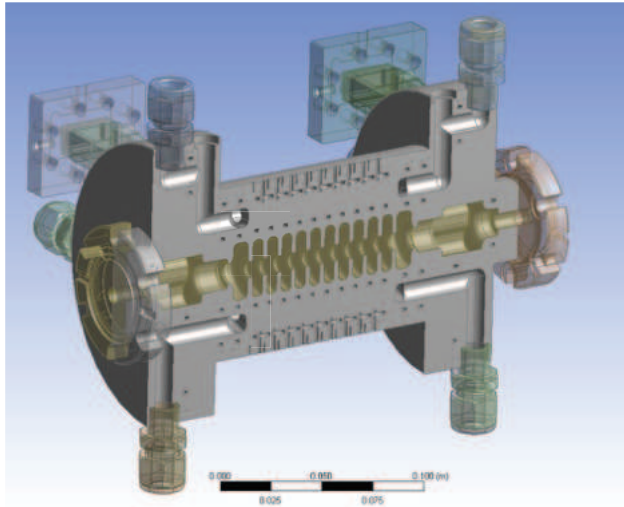


Figure 6: Mechanical drawing of a short version of the TDS constituted by 10 cells.

A first undulator prototype is arrived at PSI in June 2018, the installation of the complete undulator line is scheduled for the period from January 2019 to March 2020. The goal is to carry out a first pilot experiment before the end of 2020, with regular user operation to start in 2021.

CONCLUSION

New important results have been achieved in the SwissFEL between May and September 2018. The linac reached its nominal electron beam energy of 5.8 GeV, first lasing with a photon energy of 9 keV and in the summer period other four pilot experiments were performed. The current system upgrade and beam development program is on track in order to start regular user operation in 2019. In the meantime the installation of the Athos soft-X-ray line is progressing well, aiming at commissioning and first pilot experiments before the end of 2020.

ACKNOWLEDGEMENTS

It is a pleasure to acknowledge the valuable contributions of all the PSI support groups towards the first user opera-

tion runs at SwissFEL. To all of them go our acknowledgments. Furthermore, I am personally indebted to Thomas Schietinger for providing me large part of the materials for the talk and manuscript.

REFERENCES

- [1] C. J. Milne *et al.*, *Appl. Sci.*, vol. 7, p. 720, 2017.
- [2] T. Schietinger, in *Proc. IPAC'18*, Vancouver, BC, Canada, Apr.-May 2018, pp. 24–28. doi:10.18429/JACoW-IPAC2018-MOZGBD1
- [3] F. Loehl *et al.*, in *Proc. LINAC'16*, East Lansing, MI, USA, Sep. 2016, pp. 22–26. doi:10.18429/JACoW-LINAC2016-MO3A01
- [4] P. Craievich *et al.*, in *Proc. LINAC'18*, Beijing, China, Sep. 2018, paper THPO115, this conference.
- [5] R. Zennaro *et al.*, in *Proc. IPAC'13*, Shanghai, China, May 2013, pp. 2827–2829.
- [6] Z. Geng *et al.*, in *Proc. LINAC'14*, Geneva, Switzerland, Aug.-Sep. 2014, pp. 1114–1116.
- [7] A. Hauff *et al.*, in *Proc. LINAC'14*, Geneva, Switzerland, Aug.-Sep. 2014, pp. 683–685.
- [8] R. Ganter (Ed.), “SwissFEL conceptual design report”, Paul Scherrer Institut, Villigen, Switzerland, Rep. 10-04, Apr. 2012.
- [9] F. Fu *et al.*, *Phys. Rev. Lett.*, vol. 114, p. 114801, 2015.
- [10] S. Bettoni *et al.*, in *Proc. IPAC'18*, Vancouver, BC, Canada, Apr.-May 2018, pp. 3401–3404. doi:10.18429/JACoW-IPAC2018-THPAK074
- [11] R. Ganter (Ed.), “Athos conceptual design report”, Paul Scherrer Institut, Villigen, Switzerland, Rep. 17-02, Sep. 2017.
- [12] E. Prat, M. Calvi, R. Ganter, S. Reiche, T. Schietinger, and T. Schmidt, *J. Synchrotron Rad.*, vol. 23, pp. 861–868, 2016.
- [13] M. Paraliev, C. Gough, S. Dordevic, and H. Braun, in *Proc. FEL'14*, Basel, Switzerland, Aug. 2014, pp. 103–106.
- [14] C. Behrens *et al.*, *Nature Communications*, vol. 5, no. 3762, Apr. 2014.
- [15] A. Grudiev, “Design of compact high power rf components at x-band”, CERN, Geneva, Switzerland, Rep. CERN-ACC-NOTE-2016-0044, May 2016.
- [16] P. Craievich *et al.*, in *Proc. FEL'17*, Santa Fe, NM, USA, Aug. 2017, pp. 491–494. doi:10.18429/JACoW-FEL2017-WEPO40
- [17] P. Craievich *et al.*, in *Proc. IPAC'18*, Vancouver, BC, Canada, Apr.-May 2018, pp. 3808–3811. doi:10.18429/JACoW-IPAC2018-THPAL068